Workspaces of planar parallel manipulators

Jean-Pierre Merlet
INRIA Sophia-Antipolis
BP 93
06902 Sophia-Antipolis Cedex
France

Clément M. Gosselin
Dép. de Génie Mécanique
Université Laval
Ste-Foy, Québec, G1K 7P4
Canada

Nicolas Mouly
INRIA Rhône-Alpes
46 Av. Felix Viallet
38062 Grenoble
France

Abstract: This paper presents geometrical algorithms for the determination of various workspaces of planar parallel manipulators. Workspaces are defined as regions which can be reached by a reference point C located on the mobile platform. First, the *constant orientation* workspace is determined. This workspace is defined as the region which can be reached by point C when the orientation of the moving platform is kept constant. Then, the *maximal* workspace, which is defined as the region which can be reached by point C with at least one orientation, is determined. The maximal workspace is also referred to as the *reachable* workspace. From the above regions, the *inclusive* workspace, i.e., the region which can be attained by point C with at least one orientation in a given range, can be obtained. Then, the *total orientation* workspace, i.e., the region which can be reached by point C with every orientation of the platform in a given range, is defined and determined. Finally, the *dextrous* workspace, which is defined as the region which can be reached by point C with any orientation of the platform, can be determined. Three types of planar parallel manipulators are used to illustrate the algorithms. Each of the workspaces will be determined for each of the types of manipulators. The algorithms developed here are useful in the design and motion planning of planar parallel manipulators.

1   Introduction

Parallel manipulators have been proposed as mechanical architectures which can overcome the limitations of serial robots [1]. Several mechanical architectures of parallel mechanisms can be found in the literature (see for instance [1]). Parallel manipulators lead to complex kinematic equations and the determination of their workspace is a challenging problem. However, the solution of this problem is very important in the design and trajectory planning of the manipulators. Some researchers have addressed the problem of the determination of the workspace of parallel manipulators [2], [3], [4],[5].

In this paper, the problem of the determination of the workspaces of planar three-degree-of-freedom parallel manipulators is addressed. Algorithms are proposed for the determination of the maximal workspace, a problem which has been elusive to previous analyses. Moreover, this leads to the definition and determination of the total orientation workspace.

Planar three-degree-of-freedom parallel manipulators are composed of three kinematic chains connecting a mobile platform to a fixed base. Different types of manipulators are obtained depending on the nature of these chains. Three types of such manipulators are now defined. The manipulator of particular interest in this study is referred to as the $3-RPR$ manipulator. In this manipulator, the mobile platform is connected to the base via three identical chains consisting of a revolute joint attached to the ground followed by an actuated prismatic joint which is connected to the platform by a revolute joint (figure 1). Only the prismatic joints are actuated. Henceforth, the center of the joint connecting the ith chain to the ground will be denoted A_i and the center of the joint connecting the ith chain to the platform will be referred to as B_i. A second type of planar parallel manipulator is the $3-RRR$ robot in which the three kinematic chains connecting the platform to the base are composed of two links and three revolute joints. The joint attached to the ground is the only actuated joint in each of the chains (figure 2). This mechanical architecture has been studied by Gosselin [6] and Ma [7] and has been mentioned by Hunt [1]. For this manipulator, the center of the joint connecting the two links of the ith chain will be referred to as M_i. Moreover, the length of the links of the ith chain will be noted l_1^i (for link A_iM_i) and l_2^i (for link M_iB_i).
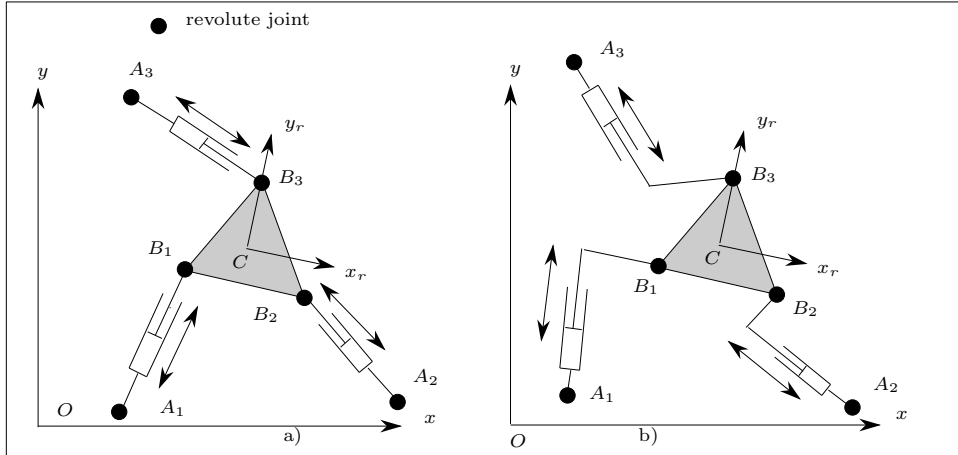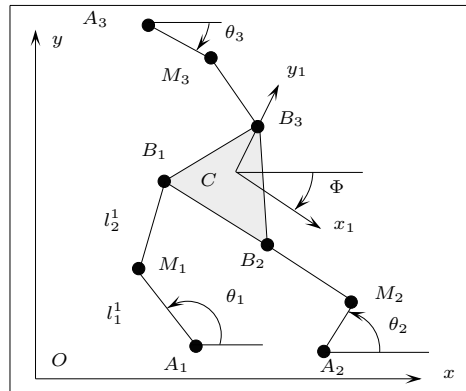
Figure 1: The $3 - RPR$ parallel manipulator.

Figure 2: The $3 - RRR$ parallel manipulator

The third type of planar parallel manipulator studied here is denoted $3 - PRR$ since each kinematic chain is constituted of a prismatic actuator fixed to the base and a link attached both to the actuator and the moving platform by revolute joints (figure 3).
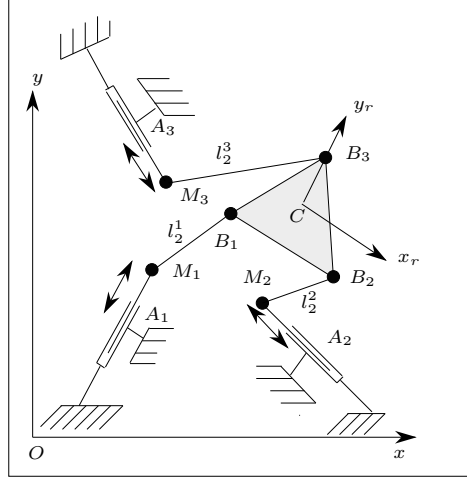

Figure 3: The $3 - PRR$ planar parallel manipulator

For each of the three manipulators, a fixed reference frame is defined on the base and a moving reference frame is attached to the platform with its origin at a reference point C. The position of the moving platform is defined by the coordinates of point C in the fixed reference frame and its orientation is given by the angle θ between one axis of the fixed reference frame and the corresponding axis of the moving frame.

For the $3 - RPR$ and $3 - PRR$ manipulators, the workspace limitations are due to the limitations of the prismatic actuators. The maximum and minimum length of the prismatic actuator of the jth chain are denoted ρ^j_{max}, ρ^j_{min}. These values will be referred to as *extreme values* of the joint coordinates. For the $3 - RRR$ manipulator, workspace limitations are either due to the geometry of the links or to some restrictions on the rotation of the revolute joints attached to the base. It is assumed here that these planar mechanisms are designed in such a way that no mechanical interference can occur between the links.

Furthermore, an *annular region* is defined as the region which lies between two concentric circles with different radii. The circle with the largest radius will be referred to as the *external circle* and the smaller circle will be referred to as the *internal circle*. The internal circle may not exist.

The dimensions of the manipulators which are used in the examples are given in the appendix. In what follows, the presentation of the various workspaces will focus on the $3 - RPR$ manipulator. Then, brief explanations on how to obtain the equivalent workspaces for the other types of planar parallel manipulators will be given.

2 Constant orientation workspace

The *constant orientation workspace* is defined as the region which can be reached by the reference point C when the moving platform has a constant orientation.

2.1 Case of the $3 - RPR$ manipulator

The algorithm for the determination of the boundary of this workspace is well known and has been described in [8] and [5].

It is first observed that for any position of C on the boundary of the workspace, at least one of link length should be at one of its extreme values. Indeed, if this condition is not met, the platform may move in any direction and therefore C cannot be located on the boundary of the workspace. Now, the region which can be reached by a point B_i is considered. This region is an annular region $\mathcal{C}_i$ whose external circle is centered at A_i with radius ρ_{max}^j and whose internal circle has the radius ρ_{min}^j. In what follows, the external circle is denoted $\mathcal{C}_i^e$ and the internal circle $\mathcal{C}_i^i$. Since the orientation is fixed, the vector $\mathbf{CB_i}$ is constant. Consequently, when B_i lies in the annular region $\mathcal{C}_i$, C also lies in an annular region $\mathcal{C}_{i_C}$ whose circles have the same radii as the circles of $\mathcal{C}_i$ but whose center is obtained by translating A_i by the vector $\mathbf{B_iC}$. If a point C lies in the workspace, then it must belong to the three regions $\mathcal{C}_{i_C}$ and therefore the workspace is the intersection of these three annular regions.

From the foregoing, it is easy to deduce that the boundary of the workspace consists of circular arcs. A very simple algorithm can be used to determine these arcs. First, all the intersection points of each of the circles belonging to the $\mathcal{C}_{i_C}$ with all the other circles are computed. Then, each circle is considered and the intersection points which have been found in the first step are ordered. The circle is therefore split into circular arcs. Each of these circular arcs is then tested, i.e., a point on the arc is used as the position of point C and the inverse kinematic problem is computed using the orientation imposed to the platform. If this computation leads to all the legs having a valid length, then the circular arc being tested is an element of the boundary of the workspace. If no intersection point is found for a given circle, a random point is taken on the circle and the condition is verified for this particular point. Examples are presented in figure 4. The orientation of the platform of the manipulator is defined as the angle between the x axis of the fixed frame and the line going from B_3 to B_1. On a SUN 4-60 workstation the
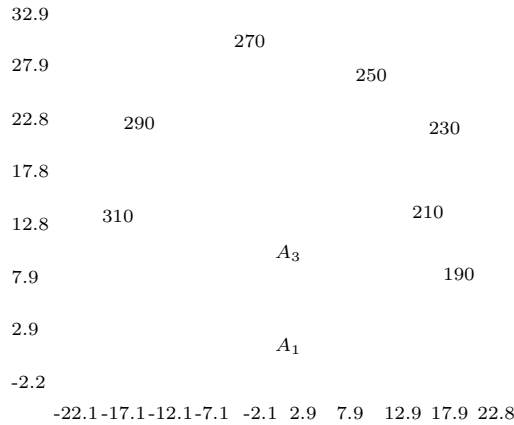

Figure 4: Examples of constant orientation workspaces for manipulator 1 of the appendix (in thin and dashed lines). The region within the thick line is the maximal workspace which will be presented in the next section. For this manipulator, the joint limits are $\rho_1 \in [8, 12]$, $\rho_2 \in [5, 15]$, $\rho_3 \in [10, 17]$

computation time for this algorithm is approximately 4-5 ms.

If the revolute joint attached to the ground cannot fully rotate, then point B_i cannot reach the full annular region $\mathcal{C}_i$ but only an angular sector of $\mathcal{C}_i$. From this sector a similar sector can be determined for C and the workspace is obtained as the intersection of the three angular sectors.

2.2 Case of the $3 - RRR$ manipulator

For this manipulator, a point B_i must lie inside an annular region $\mathcal{C}_i$ whose center is A_i with radii $l_1^i + l_2^i$ and $|l_1^i - l_2^i|$. As was the case for the $3 - RPR$ manipulator, point C is consequently inside an annular region which is obtained by translating $\mathcal{C}_i$ by vector $\mathbf{B_i C}$. The workspace is therefore the intersection of the three annular regions. In order to compute this intersection the algorithm described in the previous section remains valid.

2.3 Case of the $3 - PRR$ manipulator

For this type of manipulator, the analysis of the region which can be reached by a point B_i leads to two different types of regions (figure 5).

- if $\rho_{max}^i - \rho_{min}^i \geq 2l_2^i$ then the reachable region will consist of a rectangle of height $\rho_{max}^i - \rho_{min}^i$ and width $2l_2^i$ topped by two half-circles of radius l_2^i (figure 5, left).

- if $\rho_{max}^i - \rho_{min}^i < 2l_2^i$ then the reachable region will consist of the same zone minus the intersection of the two circles of radius l_2^i centered in $z = \rho_{max}^i, z = \rho_{min}^i$, z being the axis of the linear actuator (figure 5, right).
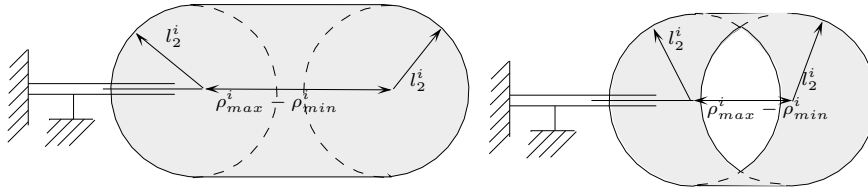

Figure 5: The reachable zone for a point B_i of a $3 - PRR$ manipulator (in grey).

The reachable regions for C are of the same type and their intersection defines the constant orientation workspace. The intersection algorithm is slightly more complex since it involves *generalized polygons*, i.e., polygons whose edges may be segments or circular arcs. A possible algorithm for computing this intersection has been described in a previous paper [4].

3 Maximal workspace

The *maximal workspace* is defined as the region which the reference point C can reach with at least one orientation. It shall be noted that the maximal workspace will depend upon the choice of the reference point.

The determination of the maximal workspace has been addressed by Kassner [9] who pointed out that the boundary of this workspace is composed of circular arcs and of portions of sextic curves. However, he was only able to compute them with a discretization method. The same observation was made by Kumar [10] but was not used in the principle of the workspace computation. Indeed Kumar uses necessary conditions on the screw motion for a point to be on the boundary of the workspace, but this method cannot be used for a manipulator with prismatic actuators.

One of the objectives of the present work is to determine geometrically the boundary of the maximal workspace.

3.1 Determining if a point is in the maximal workspace

3.1.1 Case of the $3 - RPR$ and $3 - RRR$ manipulator

First, a simple algorithm is derived to determine if a location of the reference point is in the maximal workspace, this being equivalent to determining if there is at least one possible orientation of the platform for this location.

For a given position of C, point B_1 can move on a circle C_B^1 with center C and radius $||\mathbf{CB_1}||$. The intersection of C_B^1 with the annular region $\mathcal{C}_1$, corresponding to the constraint for leg 1, is computed. If there is no intersection, circle C_B^1 is entirely located either inside or outside region $\mathcal{C}_1$. This can be determined easily by choosing a point at random on circle C_B^1 and testing if this point is inside $\mathcal{C}_1^e$ and outside $\mathcal{C}_1^i$. If this condition is satisfied, then any orientation is allowed for the platform, with respect to the constraints on leg 1. If the point is outside $\mathcal{C}_i$ then no orientation is allowed for the platform and C is outside the maximal workspace.

It is now assumed that some intersection points between C_B^1 and $\mathcal{C}_1^e$, $\mathcal{C}_1^i$ have been found. For each of these intersection points there is a unique orientation angle possible for the platform. These angles are ordered in the interval $[0, 2\pi]$ in order to obtain a set of consecutive intervals. Then, in order to determine which intervals define valid orientations for the platform, the middle value of each interval is used as the orientation of the platform and the constraints on leg 1 are tested for the corresponding configuration. A similar procedure is performed for the legs 2 and 3. For leg i, various intervals are obtained and the set I_n^i of possible orientations of the platform with respect to the constraint on the leg can be determined (figure 6). The intersection $I_\cap$ of these lists is then determined by computing the intersection of all the
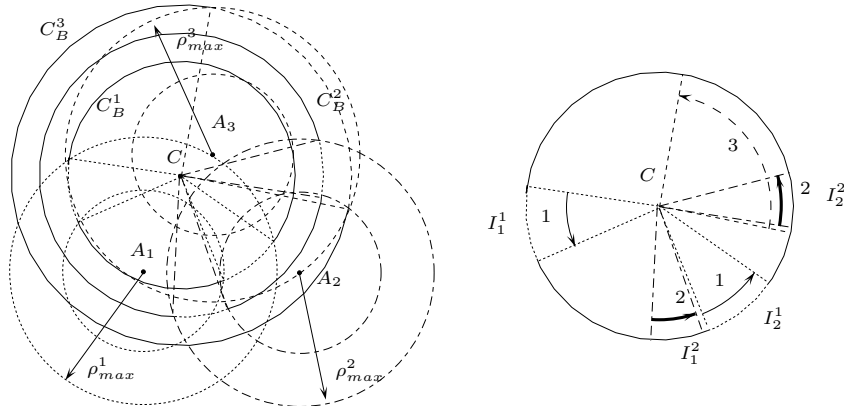

Figure 6: For a given position of C the regions which can be reached by the B_i's define three lists $\{I_l^1\}, \{I_m^2\}, \{I_n^3\}$ of intervals for the orientation of the moving platform. If C is in the maximal workspace the intersection of these lists must be non empty. On the right it may be seen that the intersection is empty as there is no intersection between $\{I_l^1\}$ and $\{I_m^3\}$.

sets of three intervals $\{I_1 \in I_n^1,\ I_2 \in I_n^2,\ I_3 \in I_n^3\}$. If $I_\cap$ is not empty then C belongs to the maximal workspace and furthermore $I_\cap$ defines the possible orientation for the moving platform at this point.

For the $3 - RRR$ manipulator, it has been shown that the constraints on the B_i's are such that B_i must lie inside an annular region. Consequently the algorithm presented above for the $3 - RPR$ manipulator also applies to the $3 - RRR$ manipulator.

3.1.2 Case of the $3 - PRR$ manipulator

The region which can be reached by the points B_i of this manipulator has been determined in section 2.3. The intersection of these regions with the circles C_B^1, C_B^2, C_B^3 is then computed. Using the intersection

points, three sets of intervals of the orientation of the platform — such that for each set the constraints on one leg are satisfied — can be determined. Once this is accomplished, the algorithm presented in the previous section can be used for the rest of the procedure.

3.2   Determination of the boundary of the maximal workspace

For purposes of simplification, it is first assumed that the reference point on the platform is chosen as one of the B_i's, for example point B_3. The general case will be presented later on as a generalization of the present discussion. If a location of B_3 belongs to the boundary of the maximal workspace then at least one of the legs is at an extreme value. Indeed, assuming that B_3 is on the boundary without satisfying this condition would mean that B_3 is capable of moving in any direction which is in contradiction with B_3 being on the boundary of the workspace. Note that the configuration with three legs in an extreme extension may define only isolated points of the boundary since they are solutions of the direct kinematics of the manipulator, a problem which admits at most 6 different solutions [11].

3.2.1   Boundary points with one extreme leg length

In order to geometrically determine the points of the boundary for which one leg length of the manipulator is at an extreme value, the kinematic chain $A_i B_i B_3$ is considered as a planar serial two-degree-of-freedom manipulator whose joint at A_i is fixed to the ground. It is well known that this manipulator is in a singular configuration when the joint centers A_i, B_i, B_3 are aligned. Consequently, the positions of B_3 belonging to the boundary of the workspace are such that A_i, B_i, B_3 lie on the same line.

   For instance, consider leg 1: two types of alignment are possible. Either $A_1 B_1 B_3$ or $A_1 B_3 B_1$ (or $B_3 A_1 B_1$) are aligned in this order as shown in figure 7. Consequently, point B_3 lies on a circle C_{B_3}
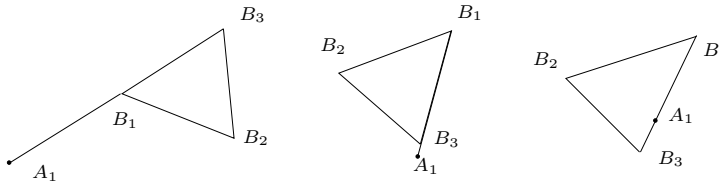

Figure 7: If a point on the boundary is such that a leg i has an extreme extension then the points A_i, B_i, B_3 are aligned.

centered at A_i. As B_3 moves on C_{B_3}, points B_1, B_2 will move on circles denoted C_{B_1}, C_{B_2}. Valid positions of B_3 on this circle are such that the corresponding positions of B_1, B_2, B_3 respectively belong to the annular regions C_1, C_2, C_3 (figure 8).

   Let α denote the rotation angle of leg 1 around A_1. The intersection points of circle C_{B_i} with the annular region C_i is then computed. All the intersection points define specific values for the angle α and the orientation of the platform. These values are ordered in a list leading to a set of intervals I^i. It is then possible to determine which intervals are components of the boundary of the workspace by taking the middle point of the arc and verifying if the corresponding pose of the platform belongs to the workspace.

   As mentioned in the previous section various types of alignment are possible and some of them will lead to a component of the boundary, i.e., the motion of the platform along some direction will be forbidden. The possible cases are:

   1. leg 1 in maximal extension, points $A_1 B_1 B_3$ aligned in this order.

   2. leg 2 in maximal extension, points $A_2 B_2 B_3$ aligned in this order.

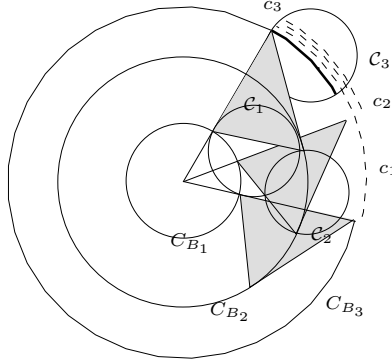   3. leg 1 in minimal extension, points $B_3 A_1 B_1$ aligned in this order.

7

Figure 8: When points A_1, B_1, B_3 are aligned, points B_1, B_2, B_3 lie on the circles $C_{B_1}, C_{B_2}, C_{B_3}$. The arcs on the circle C_{B_3} such that all the B_i belongs to the annular regions $\mathcal{C}_i$ can be components of the maximal workspace boundary. The valid arcs of C_{B_3} for a given B_i are shown in dashed lines and denoted c_i. The arcs for which all the constraints are satisfied are shown in thick lines.

4. leg 2 in minimal extension, points $B_3 A_2 B_2$ aligned in this order.

5. leg 1 in minimal extension, points $A_1 B_3 B_1$ aligned in this order.

6. leg 2 in minimal extension, points $A_2 B_3 B_2$ aligned in this order.

7. leg 1 in maximal extension, points $B_3 A_1 B_1$ aligned in this order.

8. leg 2 in maximal extension, points $B_3 A_2 B_2$ aligned in this order.

The arcs which are obtained after studying these different cases are placed in an appropriate structure and will be denoted *phase 1 arcs*.

3.2.2 Boundary points with two extreme leg lengths

The case for which the reference point lies on the boundary of the workspace while two leg lengths of the manipulator are in an extreme extension is now investigated. Since the reference point is point B_3, only the cases where the legs with extreme lengths are legs 1 and 2 needs to be considered.

When legs 1 and 2 have a fixed length, the trajectory of point B_3 is the coupler curve of a four-bar mechanism (figure 9). This mechanism has been well studied [12]·[13]·[14] and it is well known that the coupler curve is a sextic. Consequently it can be deduced that the boundary of the maximal workspace will be constituted of circular arcs and of portions of sextics.

Four sextics will play an important role in this study. They are the coupler curves of the four-bar mechanisms with lengths (r, s) (figure 9) corresponding to the various combinations of extreme lengths for legs 1 and 2, i.e., $(\rho_{max}^1, \rho_{max}^2)$, $(\rho_{max}^1, \rho_{min}^2)$, $(\rho_{min}^1, \rho_{min}^2)$, $(\rho_{min}^1, \rho_{max}^2)$.

Some particular points, referred to as the *critical points* will determine the circular arcs and the portions of sextic which define the boundary of the maximal workspace. The critical points can be of five different types, thereby defining five sets of such points.

The first set consists of the intersection points of the sextics and the annular region $\mathcal{C}_3$: in this case the three leg lengths are at an extreme value. Therefore, knowing these extreme values, these points are solutions of the *direct kinematics* problem [15]. This problem can be solved numerically and is known to lead to at most 6 solutions [11].

The second set of critical points consists of the intersection points of the sextics with the phase 1 arcs. In this case the length of legs 1 and 2 are defined by the sextics and the length of leg 3 is the radius of the arc. Consequently, these points can also be obtained from the solution of the direct kinematic problem.
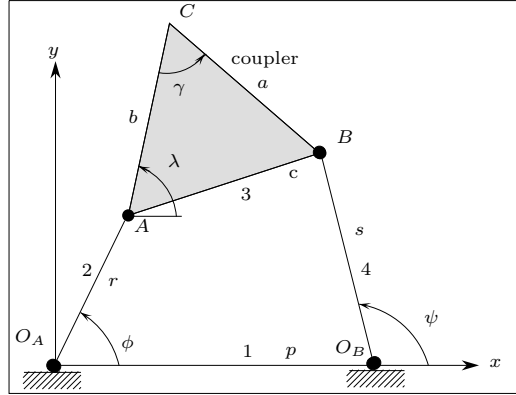
Figure 9: The four-bar mechanism.

This problem is solved and the points which belong to the arcs are retained. These points will also be critical points for the arcs.

A third set of critical points are the multiple points of the sextics. Finding these multiple points is a well known problem (see for instance Hunt [14]). In general, there are at most four double points and no triple point.

The fourth set of critical points for the sextics will be the limit points of the coupler curve. Indeed, for some value of the leg lengths the four-bar mechanism may not be a crank, i.e., the angle ϕ is restricted to belong to some intervals. Each position of B_3 corresponding to one of the bounds of the intervals is a critical point.

The last set of critical points for the sextics consists of the set of intersection points between the sextics. Determining the intersection of two coupler curves is a difficult problem. Recently Innocenti has proposed an algorithm to solve this problem [16]. It can be shown that in the general case there will be at most 18 real intersection points and in Innocenti's method these points are obtained by solving an 18th degree polynomial. However, it is pointed out that, in the present case, the coupler curves are obtained for four-bar mechanism which differ only by the lengths r, s. In this particular case it can be shown that there will be at most 12 real intersection points. Moreover, Innocenti's algorithm is difficult to implement, not very robust and time consuming. Therefore a simpler numerical algorithm has been used here.

3.2.3 Determination of the portions of sextic belonging to the boundary

Any portion of sextic belonging to the boundary must lie between two critical points. For each critical point T_i the unique pair of angles ϕ_i, ψ_i corresponding to T_i is determined. For a given value of ϕ, there are in general two possible solutions for ψ which are obtained by solving a second order equation in the tangent of the half-angle of ψ.

First, the T_i's are sorted according to the expression which is used for determining the corresponding angle ψ_i, thereby giving rise to two sets of T_i's. Each of these sets is then sorted according to an increasing value of the angle ϕ. Consequently, the sextics are split into *arcs* of sextics, some of which are components of the boundary of the maximal workspace (figure 10). A component of the boundary will be such that for any point on the arc a motion along one of the normals to the sextic will lead to a violation of the constraints while a motion along the other normal will lead to feasible values for the link lengths. Any other combination implies that the arc is not a component of the boundary of the maximal workspace. In order to perform this test, the inverse jacobian matrix for the middle point on the arc is computed as well as the unit normal vectors $\mathbf{n}_1, \mathbf{n}_2$ of the sextic at this point. Then the joint velocities are calculated for a cartesian velocity directed along $\mathbf{n}_1, \mathbf{n}_2$. The sign of the joint velocities obtained indicates whether or
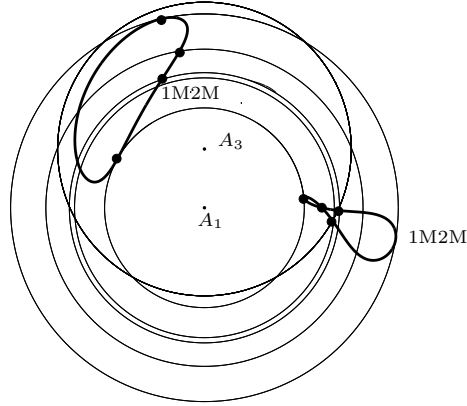
Figure 10: Point B_3 lies on a sextic when two leg lengths are at an extreme value. This sextic (in thick lines) is split into arcs between critical points. Some of these arcs will be a component of the boundary of the maximal workspace.

not the arc is a component of the boundary. For instance, for a sextic corresponding to a maximal value of the lengths of links 1 and 2, if the joint velocities $\dot{\rho}_1, \dot{\rho}_2$ are both positive for a cartesian velocity along $\mathbf{n}_1$ and both negative for a cartesian velocity along $\mathbf{n}_2$, then this arc of sextic is part of the boundary. A similar procedure is used to identify the circular arcs which are components of the boundary. To this end, the phase 1 arcs, for which the critical points — the intersection points with the sextics and the extreme points of the arcs — have been determined, are considered. Every arc between two critical points is examined to determine if the arc is a component of the boundary by using the same test as for the arcs of sextic. The boundary of the maximal workspace is finally obtained as a list of circular arcs and portions of sextics.

3.2.4   Exception

In general, for a given value of angle ϕ of a four-bar mechanism, there exist at most two possible values for angle ψ. However, if $p = r$, $\phi = 0$ and $c = s$, then angle ψ can assume any value in the interval $[0, 2\pi]$. Consequently in this case the sorting algorithm presented above must use the values of angle ψ instead of angle ϕ.

3.2.5   Examples

The maximal workspace of the manipulators described in the appendix are shown in figures 11,12,13.

3.2.6   Reachable regions

Any arc of circle obtained from the phase 1 arcs is necessarily either a component of the boundary or is rejected. None of them can be fully inside the maximal workspace. This is not true for the arcs of sextics and some of them will be eliminated because they are fully inside the maximal workspace.

Some of these arcs will exhibit an interesting feature. If the intervals for the orientation of the moving platform in the neighborhood of the arc are examined, it is possible that one of the intervals will vanish when crossing the arc. If the arc splits the maximal workspace into two parts and if the initial assembly of the manipulator is such that its orientation belongs to the interval which vanishes when crossing the arc, then the part of the workspace to which the initial assembly belongs is in fact the maximal workspace *for this initial assembly*. Any point in the other part of the workspace cannot be reached without disassembling the robot. Therefore, for each of the internal arcs of sextic whose extreme points
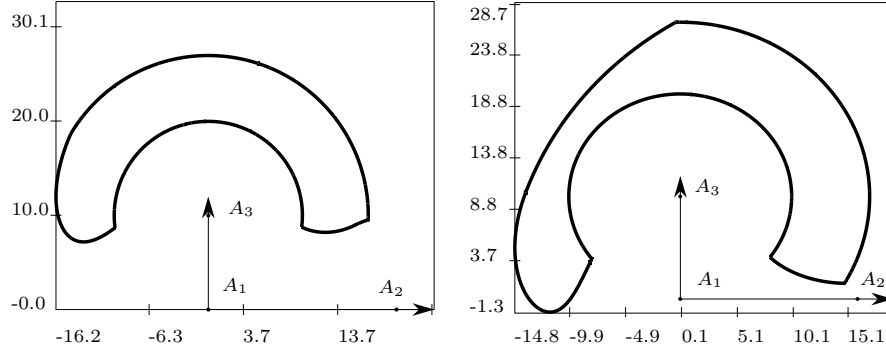
Figure 11: On the left: the maximal workspace for manipulator 1 with $\rho_1 \in [8,12]$, $\rho_2 \in [5,15]$, $\rho_3 \in [10,17]$(computation time: 4216ms). On the right: the maximal workspace for manipulator 2 with $\rho_1 \in [8,12]$, $\rho_2 \in [5,15]$, $\rho_3 \in [10,17]$(computation time: 5699ms).
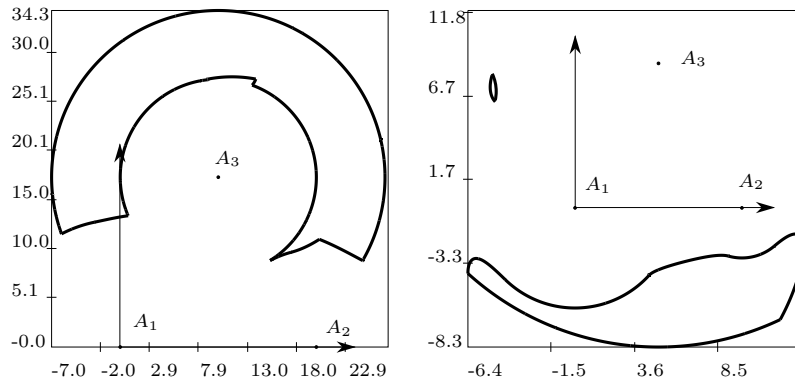

Figure 12: On the left: the maximal workspace for manipulator 3 with $\rho_1 \in [8,12]$, $\rho_2 \in [5,15]$, $\rho_3 \in [10,17]$(computation time: 14016ms). On the right: the maximal workspace for manipulator 4, $\rho_1 \in [8,12]$, $\rho_2 \in [5,15]$, $\rho_3 \in [10,17]$(computation time: 1983ms).
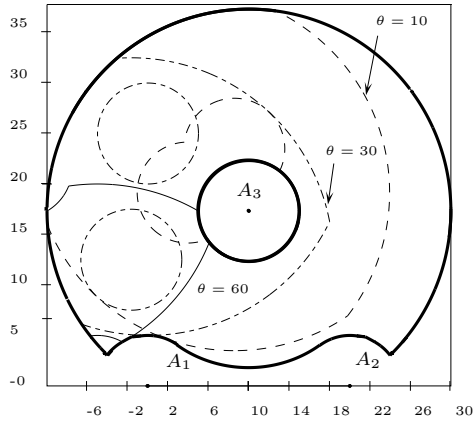
Figure 13: The area within the thick lines is the maximal workspace of manipulator 3 with $\rho_1 \in [5, 20]$, $\rho_2 \in [5, 20]$, $\rho_3 \in [5, 20]$. The dashed and thin lines represent the constant orientation workspace for various orientations of the platform.

are on the boundary of the workspace, the interval of orientation is examined by taking a random point on the arc and computing the orientation intervals for points on both side of the arc, in the vicinity of the arc. If one of the intervals vanishes on the arc then the arc is labeled as a *separating arc* which may be a component of the maximal workspace for an initial assembly of the manipulator. Figure 14 shows an example of a separating arc.
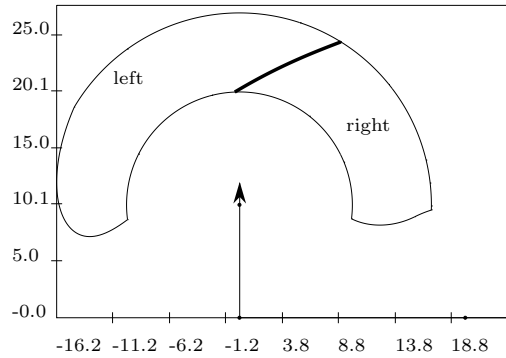

Figure 14: . The maximal workspace of a manipulator is in fact not necessarily its maximal workspace for any initial assembly. The separating arcs of the sextics allow the determination of the real maximal workspace. Here, a manipulator has been initially assembled with point B_3 positioned at (7,20) and with an orientation $\theta = 270°$. For this initial assembly, the maximal workspace is the portion of the total maximal workspace to the right of the thick line. For the initial orientation $\theta = 225°$ the maximal workspace is the total workspace (manipulator 1, $\rho_1 \in [8, 12]$, $\rho_2 \in [5, 15]$, $\rho_3 \in [10, 17]$).

3.2.7 Computation time

The computation time of the boundary of the maximal workspace is heavily dependent on the result. On a SUN 4-60 workstation this time may vary from 1500 to 15000 ms. The most expensive part of the procedure is the calculation of the intersection of the sextics.

3.2.8 Maximal workspace for any reference point

In the above discussion, it was assumed that the reference point was located on point B_3. To compute the maximal workspace for any reference point, a similar algorithm can be used. Basically, only the complexity of the algorithm will be increased. Indeed, not only the eight circles of type C_1, C_2 have to be considered but also the four circles centered at A_3 which correspond to the case where the length of link 3 has an extreme value. Similarly, only the four sextics which are obtained from the extreme values of the length of links 1 and 2 have been considered in the previous section. However, the twelve sextics which can be obtained from all the possible values for the extreme lengths of links 1, 2, 3 must now be considered. Hence, all the algorithms presented above can be applied to the general case.

3.3 Case of the $3 - RRR$ manipulator

The determination of the maximal workspace of this manipulator can performed using the algorithm described above. Indeed, the procedure is identical with the exception that the extreme values of the leg lengths are replaced by the sum and the difference of the link lengths on each of the legs. Additionally, it is pointed out that the simple algorithm based on the intersection of annular regions presented in [5] is incomplete because it does not take into account the portions of the boundary which are obtained when two legs are at one of their limits (portions of sextics).

3.4 Case of the $3 - PRR$ manipulator

Similarly to the $3 - RPR$ manipulator, a point will lie on the boundary of the workspace if at least one of the prismatic joints is at an extreme value.

If only one leg is at an extreme value, point B_3 will be on the boundary of the workspace if and only if points M_i, B_i, B_3 are aligned. Point B_3 then belongs to a circle centered in M_i (figure 15). If two prismatic
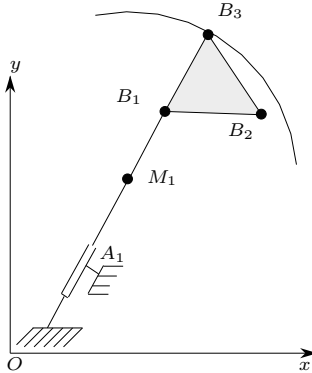

Figure 15: If only one leg is at an extreme value and B_3 is on the boundary of the maximal workspace then points M_i, B_i, B_3 are aligned. Point B_3 is therefore located on a circle centered in M_i.

joints are at an extreme value, then point B_3 lies on the coupler curve of a four-bar mechanism whose joint centers are points M_1 and M_2. Therefore, the algorithm developed for the $3 - RPR$ manipulator can also be applied to the $3 - PRR$ manipulator.

4 Inclusive maximal workspace

The *inclusive workspace* is defined as the set of all the positions which can be reached by the reference point with at least one orientation of the platform in a given interval referred to as the *orientation interval*.

This workspace will be denoted `IMW`. Hence, the maximal workspace is simply a particular case of `IMW` for which the prescribed orientation interval is $[0, 2\pi]$. In what follows, it is assumed that the orientation of the moving platform is defined by the angle between the x axis and the line B_3B_1. Moreover, it is also assumed that the reference point of the moving platform is B_3.

4.1 Case of the $3 - RPR$ manipulator

The computation of the boundary of the `IMW` is similar to the computation of the boundary of the maximal workspace. First, it is recalled that it is simple to determine if a point belongs to the `IMW` since one can compute the possible orientations of the moving platform at this point. It is also clear that a point lies on the boundary if and only if at least one of the link lengths is at an extreme value.

Consider first the circles described by B_3 when points A_i, B_i, B_3 lie on the same line. For each position of B_3 on the circles, the orientation of the moving platform is uniquely defined. The valid circular arcs must satisfy the following constraints:

- the points B_1, B_2, B_3 lie inside the annular regions $\mathcal{C}_1, \mathcal{C}_2, \mathcal{C}_3$.

- the orientation of the moving platform belongs to the orientation interval.

The determination of these arcs is thus similar to obtaining the arcs when computing the maximal workspace boundary. The main difference is that building the I^i intervals involves the consideration of the rotation angle α such that the orientation of the moving platform corresponds to one of the limits of the orientation interval.

Similarly, when the sextics are considered, the positions of B_3 for which the orientation of the moving platform is at one of the limits of the orientation interval will be added in the set of critical points.

To verify if a particular arc is a component of the boundary, the orientation for a point taken at random on the arc is examined to determine if it belongs to the orientation interval. Then the test using the inverse jacobian matrix allows to determine if the arc is a component of the boundary.

Typically the computation time for an `IMW` is about 1000 to 2000 ms on a SUN 4-60 workstation. Figures 16,17 present some `IMW` for various orientation intervals.

4.2 Case of the $3 - RRR$ manipulator

As mentioned before, the maximal workspace of the this type of manipulator is very similar to the maximal workspace of the $3 - RPR$ manipulator. Hence, the same conclusion can be drawn for the `IMW` and its determination can be performed using the algorithm proposed in the preceding subsection. The minimum and maximum lengths of the legs are substituted by the sum and difference of the link lengths on each of the legs.

4.3 Case of the $3 - PRR$ manipulator

Again, the procedure resembles the procedure outlined above for the $3 - RPR$ manipulator. It is required to take into account the orientation intervals in the computation of the phase 1 arcs and the portions of sextics.

5 Total orientation workspace

This section addresses the problem of determining the region reachable by the reference point with all the orientations in a given set $[\theta_i, \theta_j]$ which will be referred to as the orientation interval. This workspace will be denoted as `TOW`.
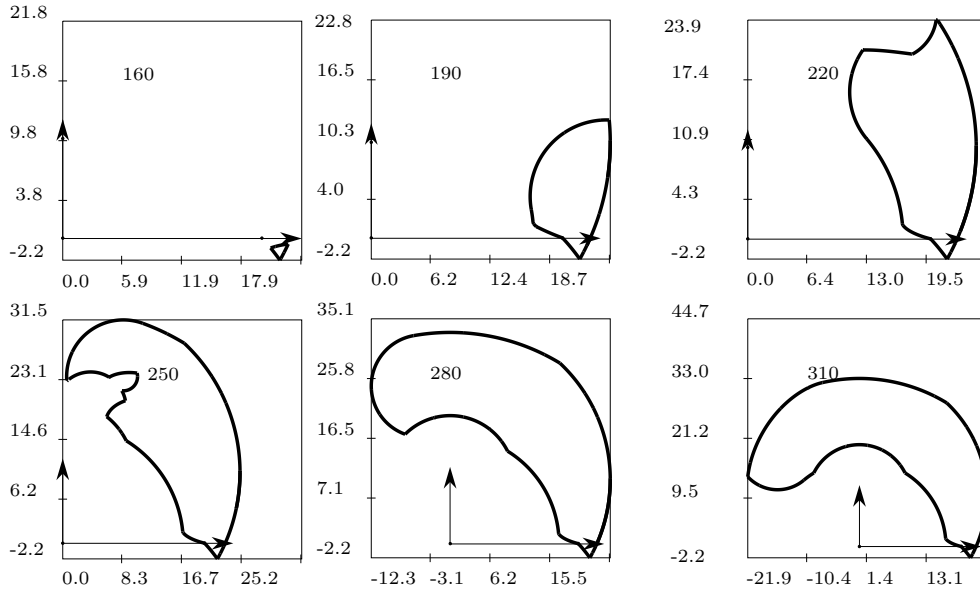
Figure 16: IMW of manipulator 1 for various orientation intervals (the orientation intervals always begin at 0). The limits are $\rho_1 \in [2, 8]$, $\rho_2 \in [5, 25]$, $\rho_3 \in [10, 25]$.
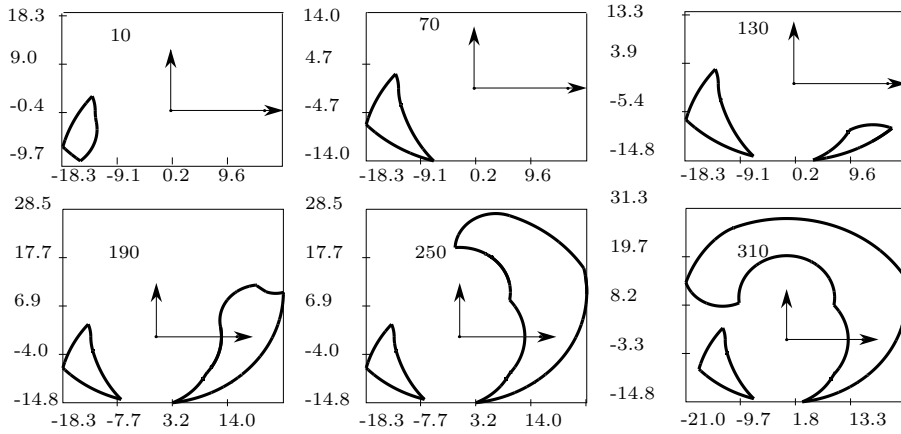
Figure 17: IMW of manipulator 2 for various orientation intervals (the orientation intervals always begin at 0). The limits are $\rho_1 \in [2, 8]$, $\rho_2 \in [5, 25]$, $\rho_3 \in [10, 25]$.

15

5.1   Case of the $3 - RPR$ manipulator

It is relatively easy to determine if a point belongs to this workspace since it is possible to compute the possible orientations for any position of the reference point. For a point belonging to the boundary of the TOW , one leg will be at an extreme value. Indeed, if a point belongs to the boundary, at least one of the legs must be at an extreme value. However, two legs cannot be at an extreme value since in that case the orientation of the moving platform is unique and consequently the point cannot belong to the TOW.

Assume that for a point on the boundary the orientation of the moving platform is one of the bounds of the interval,i.e., θ_i or θ_j while the length of leg i is at an extreme value. As B_i moves on the circle of the annular region $\mathcal{C}_i$ corresponding to the value of the leg length, point B_3 moves on a circle C_w^i with the same radius whose center is obtained by translating the center of $\mathcal{C}_i$ by the vector $\mathbf{B_i B_3}$, which is fixed since the orientation of the moving platform is known. Any point in the TOW must lie within the circle C_w^i. Therefore if the bounds θ_i, θ_j and all the possible B_i's are considered, any point of the TOW must be inside the 12 circles with center and radii $(A_3, \rho_{max}^3), (A_3, \rho_{min}^3),$ $(A_1 + \mathbf{B_1 B_3}, \rho_{max}^1), (A_1 + \mathbf{B_1 B_3}, \rho_{min}^1),$ $(A_2 + \mathbf{B_2 B_3}, \rho_{max}^2), (A_2 + \mathbf{B_2 B_3}, \rho_{min}^2).$

Assume now that a point on the boundary is reached with an orientation different from θ_i, θ_j and that the length of link 1 has an extremal value, say ρ_{max}^1. When the orientation of the moving platform lies in the orientation interval, B_1 belongs to an arc of circle defined by its center B_3, its radius $||\mathbf{B_3 B_1}||$ and the angles θ_i, θ_j. As the point belongs to the TOW the arc must lie inside the annular region $\mathcal{C}_1$. Furthermore this arc is tangent at some point to the external circle of $\mathcal{C}_1$ since B_3 lies on the boundary of the TOW (figure 18). This tangency implies that point B_3 lies on a circle of center A_1 and radius $\rho_{max}^1 - ||\mathbf{B_1 B_3}||$.
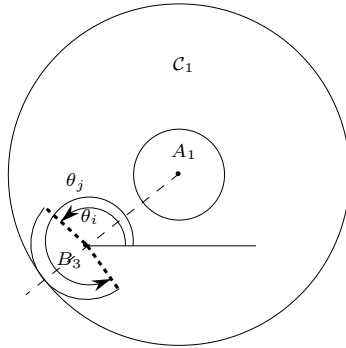

Figure 18: Point B_3 belongs to the boundary of the TOW with the length of link 1 being ρ_{max}^1. Consequently B_1 lies on a circular arc with center B_3, radius $||\mathbf{B_3 B_1}||$ and angles θ_i, θ_j. This arc must be included in the annular region $\mathcal{C}_1$ and is tangent at some point to the external circle of $\mathcal{C}_1$.

Any point within the TOW must be inside this circle. Four such circles may exist, whose center and radii are $(A_1, \rho_{max}^1 - ||\mathbf{B_1 B_3}||), (A_1, \rho_{min}^1 - ||\mathbf{B_1 B_3}||), (A_2, \rho_{max}^2 - ||\mathbf{B_2 B_3}||), (A_2, \rho_{min}^2 - ||\mathbf{B_2 B_3}||).$

If a point B_3 belongs to the TOW it is necessary that the point is included in the 16 circles which have been determined. Consequently the boundary of the TOW is the intersection of these sixteen circles. Note that for the last four circles, theoretically only the arcs for which the orientation of the moving platform is inside the orientation interval have to be considered. However, such arcs will be determined by the intersection of the circle with some of the initial twelve circles. The intersection algorithm described in the section devoted to the constant orientation workspace can be used to determine the intersection of the circles.

Figures 19,20 illustrate some examples of TOW. The computation time is approximately 100 ms on a SUN 4-60 workstation.
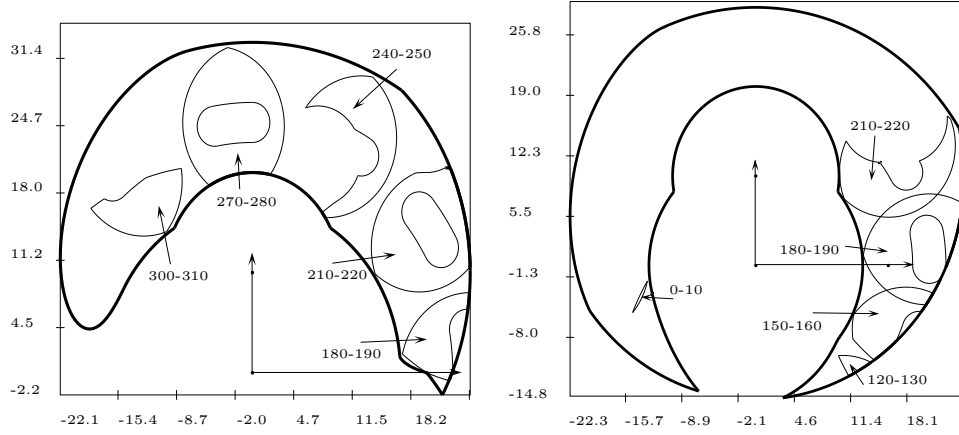
Figure 19: Examples of total orientation workspaces for manipulators 1 and 2 with $\rho_1 \in [2, 8]$, $\rho_2 \in [5, 25]$, $\rho_3 \in [10, 25]$.
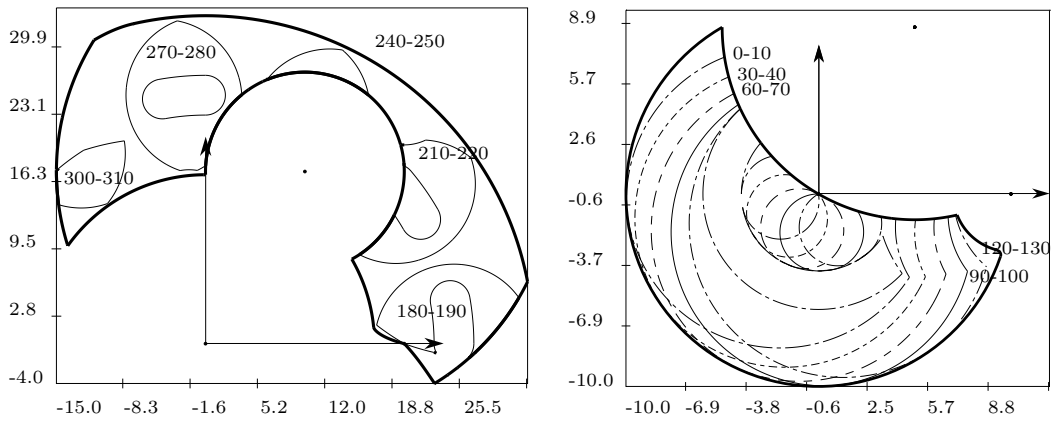

Figure 20: Examples of total orientation workspaces for manipulators 3 and 4 with $\rho_1 \in [2, 8]$, $\rho_2 \in [5, 25]$, $\rho_3 \in [10, 25]$.

5.2   Case of the $3-RRR$ manipulator

The same algorithm is used with ρ^i_{max} replaced by $l^i_1 + l^i_2$ and ρ^i_{min} by $|l^i_1 - l^i_2|$.

5.3   Case of the $3-PRR$ manipulator

Let A^M_i, A^m_i be the extreme positions of point M_i. The regions which will be used in the algorithm are

- the reachable region of B_3

- circles with center A^M_1, A^m_1 + $\mathbf{B_1B_3}$, radius l^1_2

- circles with center A^M_2, A^m_2 + $\mathbf{B_2B_3}$, radius l^2_2

The last two items are obtained for an orientation of the moving platform equal to one of the bounds of the orientation interval. For a fixed position of A_i when the orientation of the moving platform lies within the orientation interval, point B_3 lies on a circle with center A_i and radius $l^i_2 - ||\mathbf{B_iB_3}||$. Consequently as A_i moves between A^M_i, A^m_i, point B_3 lies inside a region composed of a rectangle whose width is equal to the range of the linear actuator and whose height is $2(l^i_2 - ||\mathbf{B_iB_3}||)$, topped by two half-circles centered at A^M_i, A^m_i with radius $l^i_2 - ||\mathbf{B_iB_3}||$ (figure 21). These regions are computed for links 1 and 2 and their
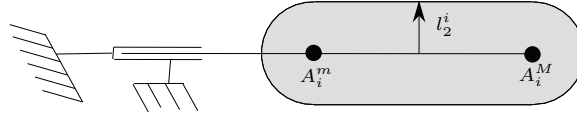

Figure 21: The region described by point B_3 when the orientation of the moving platform describes the orientation interval.

intersection with the region reachable by B_3 defines the TOW.

6   Dextrous workspace

The *dextrous workspace* is the region which can be reached by the reference point with any orientation. Note that the dextrous workspace is a particular case of TOW.

Kumar [2] has used screw theory to determine the boundary of the dextrous workspace for the $3-RRR$ manipulator. However, his method cannot be used for manipulators with linear actuators and cannot be easily modified to take into account the mechanical limits on the joints. In [5] and [3], geometrical algorithms for the determination of the dextrous workspace of a $3-RRR$ manipulator have been presented. The algorithm presented in this section is similar to these algorithms.

6.1   Case of the $3-RPR$ manipulator

Let C_1 be a point belonging to the dextrous workspace. Since any orientation of the moving platform is allowed, any B_i belonging to the circle centered in C_1 with radius $||\mathbf{CB_i}||$ has to lie inside the annular region $\mathcal{C}_i$. Consequently C_1 must belong to the annular region CA_i centered in A_i whose radii are $\rho^i_{min} + ||\mathbf{CB_i}||$ and $\rho^i_{max} - ||\mathbf{CB_i}||$. This annular region will exist if and only if $\rho^i_{max} - \rho^i_{min} \geq 2||\mathbf{CB_i}||$ (figure 22). Therefore the dextrous workspace is the intersection of the three regions CA_i. Figure 23 shows an example of dextrous workspace. Mechanical limits on the joints can easily be included in this algorithm.
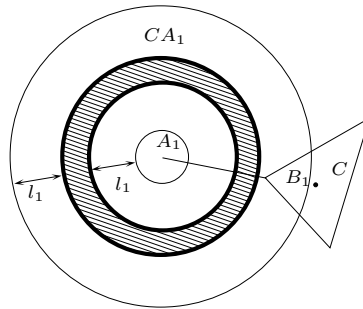
Figure 22: The dextrous workspace for C if only the constraint on link 1 are taken into account.
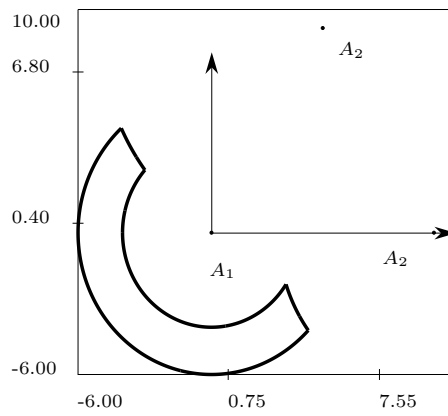

Figure 23: Dextrous workspace for manipulator 4 ($\rho_1 \in [2,8]$, $\rho_2 \in [5,25]$, $\rho_3 \in [10,25]$, computation time: 80ms).

6.2 Case of the $3 - RRR$ manipulator

Similarly to the $3 - RPR$ manipulator, points B_i must be included in an annular region $\mathcal{C}_i$. Consequently the possible region for C with respect to the constraint on link i is the annular region CA_i centered in A_i whose circles radii are $|l_2^i - l_1^i| + ||\mathbf{CB_i}||$ and $l_1^i + l_2^i - ||\mathbf{CB_i}||$. This region will exist if and only if $l_1^i + l_2^i > ||\mathbf{CB_i}||$ and $l_1^i + l_2^i - |l_2^i - l_1^i| > 2||\mathbf{CB_i}||$. The dextrous workspace is the intersection of the three regions CA_i. This algorithm is similar to the one presented in [5].

6.3 Case of the $3 - PRR$ manipulator

In the section devoted to the constant orientation workspace, the region which can be reached by the points B_i was computed. Therefore the possible positions for C must be determined such that a circle centered in C with radius $||\mathbf{CB_i}||$ is fully inside the reachable region for B_i. A simple geometrical reasoning allows to show that such a region will exist if and only if $l_2^i > ||\mathbf{CB_i}||$. There are two possible types for this region (figure 24):

- if $\rho_{max}^i - \rho_{min}^i > 2l_2^i$: a rectangle of height $\rho_{max}^i - \rho_{min}^i$ and width $2(l_2^i - ||\mathbf{CB_i}||)$ topped by two half-circles with radius $l_2^i - ||\mathbf{CB_i}||$ (figure 24, left)

- if $\rho_{max}^i - \rho_{min}^i < 2l_2^i$: the intersection of two circles centered in $z = \rho_{max}^i$ with radius $l_2^i - ||\mathbf{CB_i}||, l_2^i + ||\mathbf{CB_i}||$ and the intersection of two circles centered in $z = \rho_{min}^i$ with same radius, z being the axis of the linear actuator (figure 24, right).
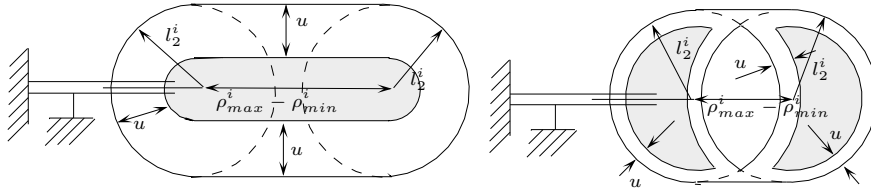

Figure 24: The dextrous workspace for C when only the constraints on link 1 are taken into account (in grey, $u = ||\mathbf{CB_1}||$).

The dextrous workspace is the intersection of these three regions and the algorithm described in [4] can be used to compute this intersection.

7 Conclusion

Geometrical algorithms for the determination of the boundary of various workspaces for planar parallel manipulators have been described. These algorithms are exact (no discretization is used) and in general their computation time is small, except for the maximal workspace.

The determination of the workspaces is very useful in the context of design or motion planning of parallel manipulators.

Acknowledgements

Appendix

The dimensions of the manipulators used in the examples of this paper are defined in figure 25 and their numerical values are presented in table 1.
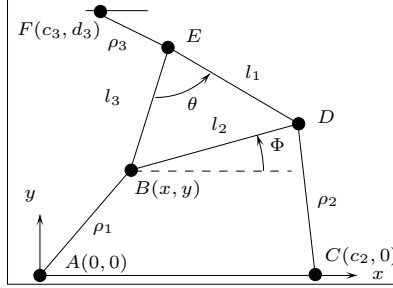

Figure 25: Definition of the dimensions of the manipulators.

Manipulator	Type	l_1	l_2	l_3	c_2	c_3	d_3	θ
1	RPR	25	25	25	20	0	10	60
2	RPR	20.839	17.045	16.54	15.91	0	10	52.74
3	RPR	25	25	25	20	10	17.32	60
4	RPR	2	2	2	10	5	8.66	60

Table 1: Dimensions of the manipulators used in the examples (all the angles are in degrees).

References

[1] Hunt K.H. Structural kinematics of in parallel actuated robot arms. *J. of Mechanisms, Transmissions and Automation in Design*, 105(4):705–712, March 1983.

[2] Kumar V. Characterization of workspaces of parallel manipulators. *ASME J. of Mechanical Design*, 114(3):368–375, September 1992.

[3] Pennock G.R. and Kassner D.J. The workspace of a general geometry planar three degree of freedom platform manipulator. *ASME J. of Mechanical Design*, 115(2):269–276, June 1993.

[4] Merlet J-P. Manipulateurs parallèles, 5eme partie : Détermination de l'espace de travail à orientation constante. Research Report 1645, INRIA, March 1992.

[5] Williams II R.L. and Reinholtz C.F. Closed-form workspace determination and optimization for parallel robot mechanisms. In *ASME Proc. of the the 20th Biennial Mechanisms Conf.*, pages 341–351, Kissimmee, Orlando, September, 25-27, 1988.

[6] Gosselin C. *Kinematic analysis optimization and programming of parallel robotic manipulators*. PhD thesis, McGill University, Montréal, June, 15, 1988.

[7] Ma O. and Angeles J. Direct kinematics and dynamics of a planar three-dof parallel manipulator. In *ASME Design and Automation Conf.*, volume 3, pages 313–320, Montréal, September, 17-20, 1989.

[8] Gosselin C. and Angeles J. The optimum kinematic design of a planar three-degree-of-freedom parallel manipulator. *J. of Mechanisms, Transmissions and Automation in Design*, 110(1):35–41, March 1988.

[9] Kassner D.J. Kinematics analysis of a planar three-degree-of-freedom platform-type robot manipulator. Master's thesis, Purdue University, Purdue, December 1990.

[10] Kumar V. Characterization of workspaces of parallel manipulators. In *ASME Proc. of the 21th Biennial Mechanisms Conf.*, pages 321–329, Chicago, September, 16-19, 1990.

[11] Gosselin C., Sefrioui J., and Richard M.J. Solution polynomiale au problème de la cinématique directe des manipulateurs parallèles plans à 3 degrés de liberté. *Mechanism and Machine Theory*, 27(2):107–119, March 1992.

[12] Artobolevski I. *Théorie des mécanismes et des machines*. Mir, Moscou, 1975.

[13] Hartenberg R.S. Denavit J. *Kinematic synthesis of linkages*. McGraw-Hill, New-York, 1964.

[14] Hunt K.H. *Kinematic geometry of mechanisms*. Clarendon Press, Oxford, 1978.

[15] Merlet J-P. *Les Robots parallèles*. Hermès, Paris, 1990.

[16] Innocenti C. Analytical determination of the intersection of two coupler-point curves generated by two four-bar linkages. In J. Angeles P. Kovacs, G. Hommel, editor, *Computational Kinematics*, pages 251–262. Kluwer, 1993.